Geophysical Research Letters

Supporting Information for

How choice of depth horizon influences the estimated spatial patterns and global magnitude of ocean carbon export flux

Hilary I. Palevsky[1], Scott C. Doney[2]

[1]Department of Marine Chemistry and Geochemistry, Woods Hole Oceanographic Institution, Woods Hole, MA, USA
[2]Department of Environmental Sciences, University of Virginia, Charlottesville, VA, USA

Contents of this file

Introduction

Figure S1 presents a comparison between depth profiles of POC flux from the model and from available observational data.

The Supplemental Text and Figure S2 provide further detail about the methods used to calculate the depth horizons for evaluating model POC flux and e-ratio.

Figure S3 presents alternative versions of Figures 2b-c from the main text, comparing results for export at the maximum annual MLD with results for each other choice of depth horizon not used for the comparison in the main text.

Figure S1. Comparison of depth profiles of POC flux (mmol C m^{-2} d^{-1}) from the CCSM-BEC model output (black lines) and previously-published POC flux profiles from observational approaches (colored dots). Note that the scale for POC flux (x-axis) varies among the profiles. Observational data from the Atlantic Ocean (Porcupine Abyssal Plain (PAP), the Irminger and Iceland Seas, and the North Atlantic Subtropical Gyre (NSAG); top row) are from neutrally buoyant sediment trap measurements [*Marsay et al.*, 2015]. Observational data from the Pacific Ocean (stations K2 and ALOHA in the northwest and eastern subtropical north Pacific, the equatorial Pacific (EQPAC), station KIWI in the Pacific sector of the Southern Ocean, and Ocean Station Papa (OSP); bottom row) are derived from ^{234}Th flux measurements [*Buesseler and Boyd*, 2009]. Sampling locations for each profile are shown in the inset map on the top right. Model data for comparison are taken from the model's corresponding spatial grid cell during the month most closely corresponding to the observational sampling, with all profiles collected during the spring-summer period (and in the case of K2, KIWI, and OSP, two different profiles were collected in a similar time period at the same location).

The comparison between model and observational data shows reasonably good correspondence both between the absolute magnitude of POC flux and shape of POC flux attenuation with depth. Mismatch between the observations and model output may reflect spatial and temporal variability captured in the observations but not represented in the model climatology, in addition to errors in the model's representation of POC flux rates. The limited number of observational profiles restricts the ability to perform a comprehensive quantitative model-observational data comparison across profiles rather than single measurements per location (as was done by *Lima et al.*, 2014), further justifying the need for additional observational sampling to improve the ability to observationally validate model studies.

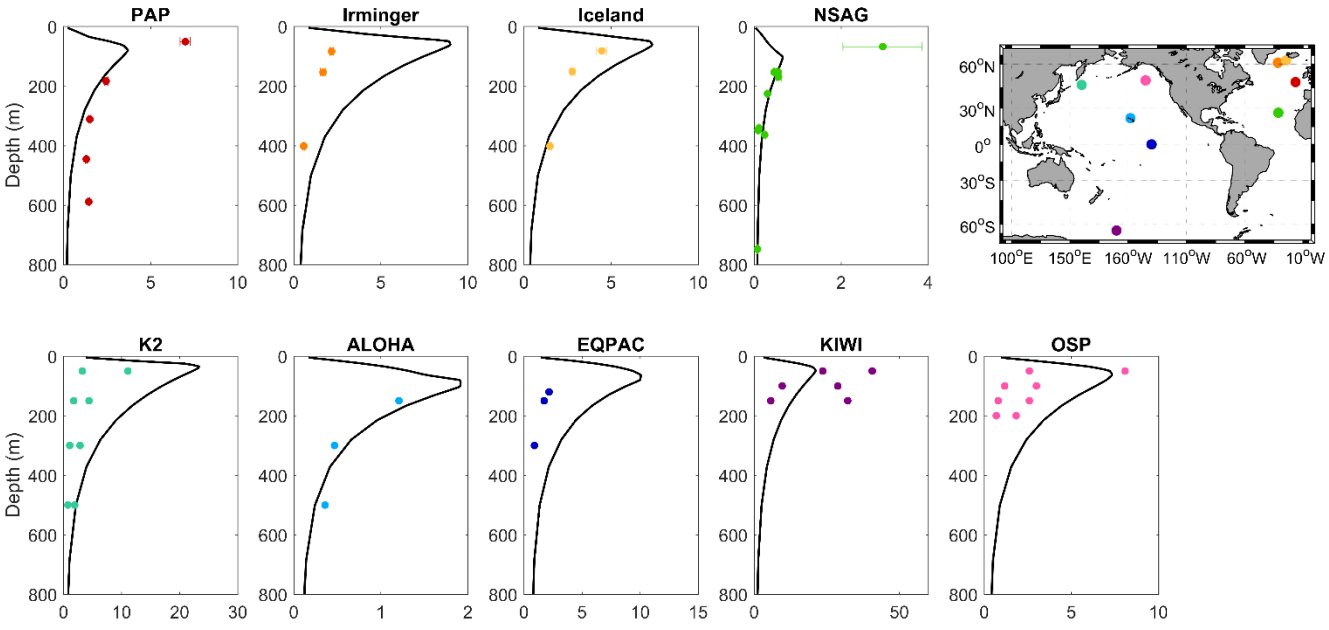

Supplemental Text: Calculation of Export Depth Horizons

Export is defined in this paper using five different depth horizons (**Table 1** in the main text) below which particulate organic carbon (POC) must "sink" in the CCSM-BEC simulation to be counted as exported in evaluating POC flux and e-ratio (POC flux/net primary production). Two of these depth horizons do not vary seasonally: the 100-meter depth horizon is a fixed depth for all grid cells in all months, and the maximum annual mixed layer depth (MLD) is defined as the deepest monthly MLD of the year for each spatial grid cell. However, three of these depth horizons – the seasonally-varying MLD, the euphotic depth, and the particle compensation depth – vary in depth throughout the year for each spatial grid cell in the model. **Figure S1** shows seasonal variability in each of these depth horizons (calculated for each month of climatological model output) for four example locations.

The base of the seasonally-varying mixed layer is determined in each month for each grid cell based on model physics. The particle compensation depth is determined in each month for each grid cell as the depth in the water column where the POC flux rate reaches its maximum. The base of the euphotic zone is calculated in each month for each grid cell following the definition previously used by Lima et al. (2014) for this model: the depth where the POC production rate attenuates to 1% of the maximum POC production rate throughout the full water column in that location. We note that this definition of the euphotic zone differs from approach most commonly used in observational studies, which instead determines the base of the euphotic zone as the depth where photosynthetically available radiation (PAR) attenuates to 1% or 0.1% of its surface value. We use the alternative definition based on POC production rate in our analysis both for consistency with previous analysis of this same model output (Lima et al. 2014), and because defining the euphotic zone based on POC production profiles is a more direct way of determining the layer in which photosynthetic production occurs, whereas PAR has been used as a field proxy due to the difficulty of measuring production rates in continuous full-depth profiles.

Annual POC flux and e-ratio across the seasonally-varying depth horizons are calculated from monthly POC flux and water-column integrated NPP rates each determined at the monthly depth horizon. In order to visualize the influence of depth horizon choice on mean annual POC flux and e-ratio (**Figure 1** in the main text), we calculate a weighted mean annual depth for each of the seasonally-varying depth horizons in each spatial grid cell. The monthly weights are calculated based on the fraction of the total annual POC flux across a given depth horizon that occurs in each month. **Figure S1** shows examples of the annual mean POC flux profile and weighted annual mean depth horizons for example locations with strong seasonal cycles in the seasonally-varying depth horizons, illustrating that the annual mean depth horizon most closely matches the seasonally-varying depth horizon during the period when the greatest POC flux occurs.

Figure S2. Seasonal variation in export depth horizons and POC flux (left) and annual mean POC flux profiles and depth horizons (right; POC flux in units of mol C m^{-2} yr^{-1}), shown for four representative locations with relatively deep winter mixing (locations shown as yellow dots in Figures 2a-b in the main text). Note that the POC flux scales and depth axes vary for each location. Annual mean depth horizons are weighted by POC flux in each month, such that the deep euphotic and particle compensation depths evident in winter do not strongly influence the annual mean value. The annual mean of the seasonal MLD horizon is obscured for the Southern Ocean because it matches the annual mean particle compensation depth.

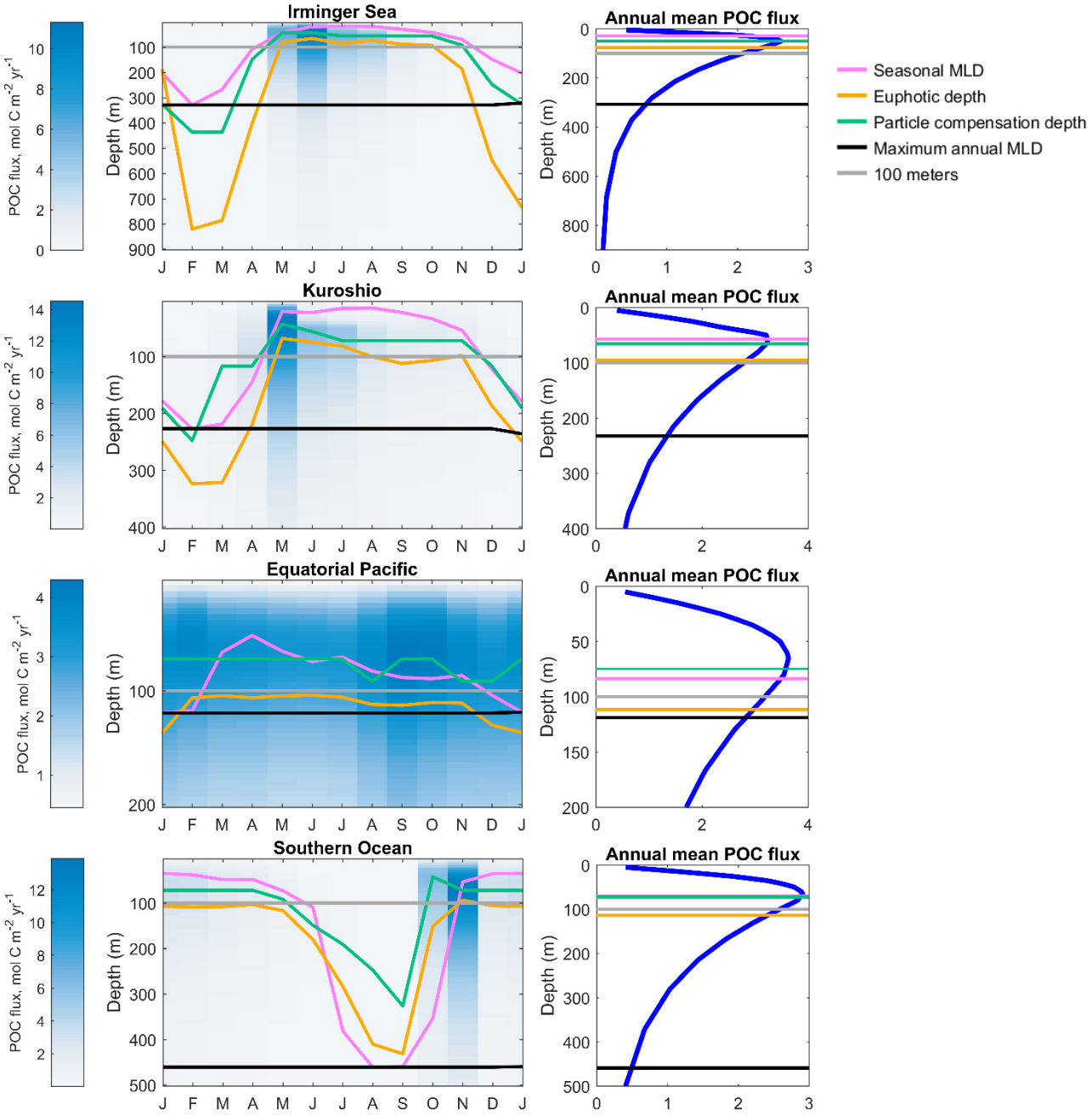

Figure S3. Alternative versions of Figures 2b-c, showing the relationship between POC flux at the maximum annual MLD depth horizon and (top) the seasonally-varying MLD, (middle) the euphotic depth, and (bottom) the particle compensation depth. Panels on the left show maps of the difference between POC flux at each given depth horizon and at the maximum annual MLD, and panels on the right show the correlation between the maximum annual MLD in each grid cell and the differences shown spatially in map view. Each point represents an individual grid cell, with points where maximum annual MLD < 60 m omitted and the colors representing overlapping point density. with using seasonal MLD for comparison.

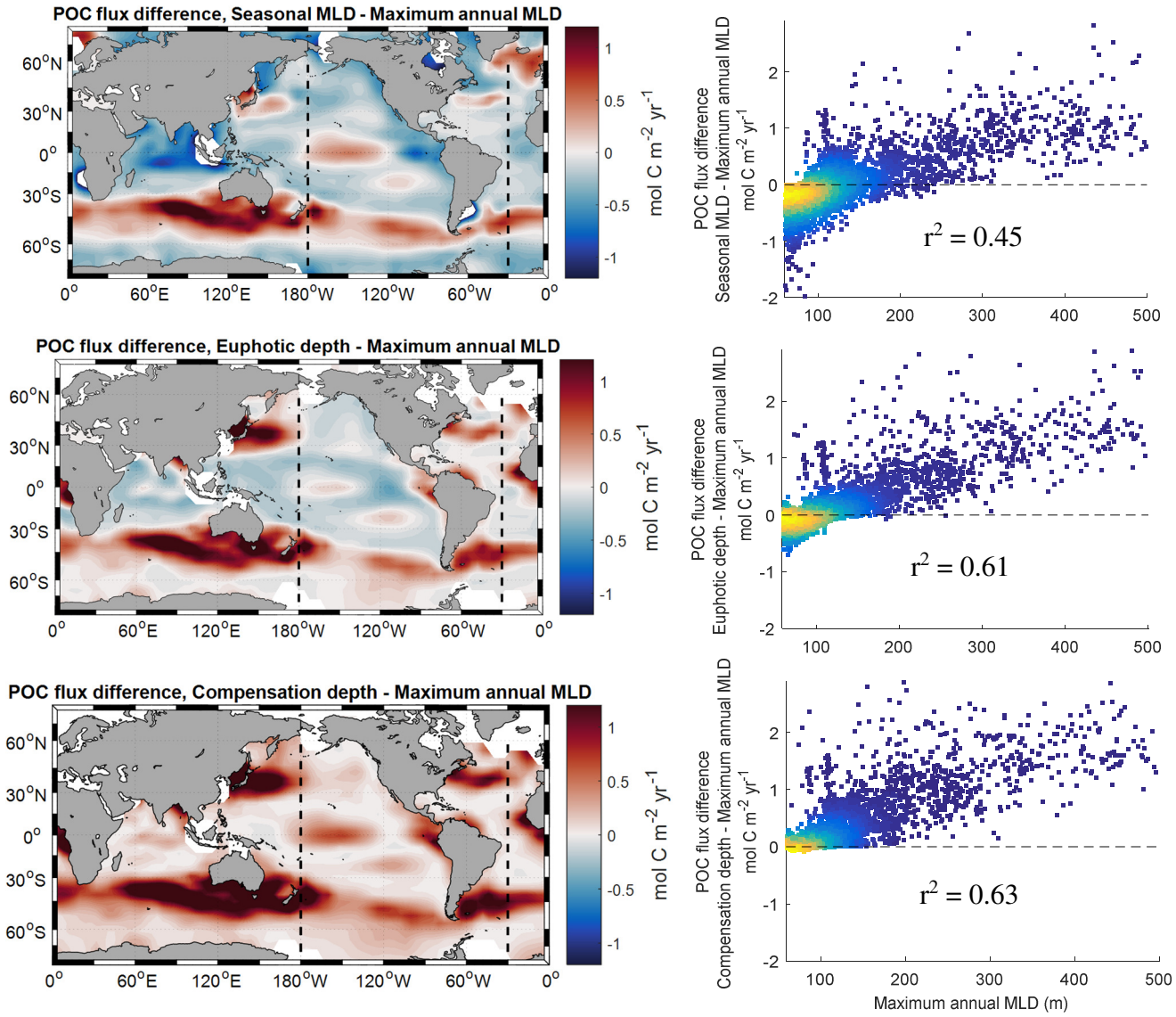

References

Buesseler, K. O., and P. W. Boyd (2009), Shedding light on processes that control particle export and flux attenuation in the twilight zone of the open ocean, *Limnol. Oceanogr.*, *54*(4), 1210–1232, doi:10.4319/lo.2009.54.4.1210.

Lima, I. D., P. J. Lam, and S. C. Doney (2014), Dynamics of particulate organic carbon flux in a global ocean model, *Biogeosciences*, *11*, 1177–1198, doi:10.5194/bg-11-1177-2014.

Marsay, C. M., R. J. Sanders, S. A. Henson, K. Pabortsava, E. P. Achterberg, and R. S. Lampitt (2015), Attenuation of sinking particulate organic carbon flux through the mesopelagic ocean, *Proc. Natl. Acad. Sci.*, *112*(4), 1089–1094, doi:10.1073/pnas.1415311112.